

# Net-Baryon Multiplicity and QCD Phase Diagram

---

## Zn Collaboration

### Ryutaro Fukuda

*Department of Physics, The University of Tokyo, Tokyo 113-0033, Japan*

### Atsushi Nakamura\*

*RIISE Hiroshima University*

*E-mail: nakamura@riise.hiroshima-u.ac.jp*

### Syotaro Oka

*Institute of Theoretical Physics, Rikkyo University Toshima-ku, Tokyo 171-8501, Japan*

### Shuntaro Sakai

*Department of Physics, Kyoto University, Kyoto 606-8502, Japan*

### Asobu Suzuki and Yusuke Taniguchi

*Graduate School of Pure and Applied Sciences, University of Tsukuba, Ibaraki 305-8571, Japan*

### Kenji Morita

*Yukawa Institute for Theoretical Physics, Kyoto University, Kyoto 606-8502, Japan*

### Keitaro Nagata

*KEK, Tsukuba 305-0801, Japan*

The net-baryon multiplicity is a link between high energy heavy ion collision experiments and lattice gauge simulations both of which are pursued hardly to find the QCD critical point. We propose to study the canonical partition function,  $Z_n$ , in both experimental and numerical studies. We first present a recipe how to extract  $Z_n$  from experimental multiplicities and apply it for the net-proton multiplicities, which can be a proxy of the net baryon multiplicity.

Next we present a method to calculate  $Z_n$  in the lattice QCD. Lattice simulations at finite density had been believed to go wrong because of the notorious sign problem. We show that a new fugacity expansion works, and we can obtain  $Z_n$  at the deconfinement region ( $T > T_c$ ) and not very low temperature region at  $T < T_c$ .

Using the relation between  $Z_n$  and the grand canonical function,  $Z$ ,

$$Z(\mu, T) = \sum_n Z_n(T) e^{n\mu/T},$$

we can evaluate both real and complex chemical potential regions, both in experiment and lattice simulations. This relation is a powerful new tool to search for the QCD critical point, both in experimental and numerical analyses.

*9th International Workshop on Critical Point and Onset of Deconfinement*

*17-21 November, 2014*

*ZiF (Center of Interdisciplinary Research), University of Bielefeld, Germany*

## 1. Introduction

Needless to say, at least to those of the CPOD society, one of the most important research goal is to clarify the QCD phase at finite temperature and density. Towards this goal, many theoretical and experimental efforts have been done:

1. Experimentally, multiplicity distributions have been measured by varying energies in high energy heavy ion collisions (BES (beam energy scan) experiments) [1, 2].
2. Phenomenologically, many interesting phases are predicted[3].
3. Numerically lattice QCD simulation is well formulated not only zero temperature and zero density, but also at extreme condition[5].

Difficulty of each approaches are the following:

1. We measure hadrons in detectors. They are travelling on the temperature-density plane after the deconfinement transition. So-called freezeout temperature and density are not on the phase transition line, but within the confinement region. They bring the information about the phase transition line, but we must extract the transition point, in some method.
2. Effective theories have usually unknown parameters, which are constrained by the symmetry. Then their predictions are varying.
3. The lattice QCD simulation at finite chemical potential suffers from the sign problem, i.e.,  $\det D(\mu)$  in the following path integral is complex,

$$Z(\mu, T) = \int \mathcal{D}U (\det D(\mu))^{N_f} e^{-S_G} \quad (1.1)$$

and the probability in the Monte Carlo step  $(\det D(\mu))^{N_f} e^{-S_G} / Z$  is complex in general.

In this report, we study the canonical approach which may solve the difficulty 1. and 3. above.

## 2. Grand Canonical Partition Function, $Z$ , vs. Canonical Partition Function, $Z_n$

We assume that fire-balls created in high energy heavy ion collision are described by the grand canonical partition function,

$$Z(\mu, T) = \text{Tr} e^{-(H - \mu \hat{N})/T}, \quad (2.1)$$

where  $\mu$  and  $T$  are the chemical potential and the temperature, respectively.  $\hat{N}$  and  $H$  are the number operator and the Hamiltonian, respectively. The system is considered to be in a equilibrium state, and therefore this is an approximation. Surprisingly this is a good approximation, since we describe the system in terms of  $\mu$  and  $T$  without much contradiction[6].

The relation between the grand canonical and canonical partition functions can be expressed as

$$Z(\xi, T) = \text{Tr} e^{-(H - \mu \hat{N})/T} = \sum_{n=-N_{max}}^{+N_{max}} \langle n | e^{-H/T} | n \rangle e^{\mu n/T} = \sum_{n=-N_{max}}^{+N_{max}} Z_n(T) \xi^n, \quad (2.2)$$

---

\*Speaker.

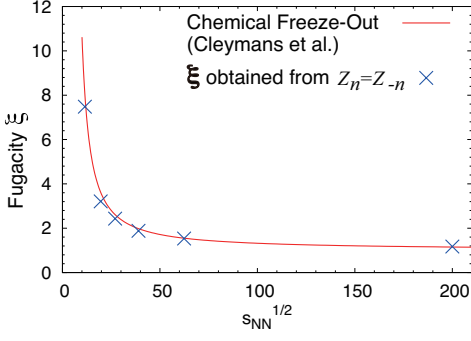


**Figure 1:** Fugacity  $\xi = \exp(\mu/T)$  as a function of collision energy  $\sqrt{s_{NN}}$ . Plotted values are those obtained from RHIC experiments (blue crosses) and the freeze-out results reported in Ref.[4].

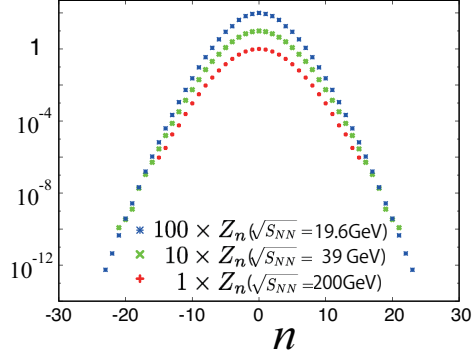


**Figure 2:**  $Z_n$  calculated from RHIC data with  $\sqrt{s_{NN}} = 19.6$  39 and 200 GeV.

where  $Z_n = \langle n | e^{-H/T} | n \rangle$  and  $\xi \equiv \exp(\mu/T)$  is the fugacity. Here, we assume that the number operator  $\hat{N}$  commutes with the Hamiltonian  $H$ , that is,  $\hat{N}$  is a conserved quantity.

From its definition, we see the following two characters of the canonical partition functions:

1.  $Z_n$  are function of the temperature  $T$ , but not the chemical potential  $\mu$ .
2.  $Z_n$  satisfies

$$Z_n = Z_{-n}, \quad (2.3)$$

due to the charge conjugation and parity symmetries.

The coefficients  $Z_n$  are canonical partition functions. The relation Eq.(2.2) is useful for investigating the QCD phase diagram because if we obtain  $Z_n$ , which is a function of the temperature  $T$ , we can calculate the grand canonical partition functions at any  $\mu/T$  for the same temperature  $T$ . See Fig.3

### 3. How to calculate $Z_n$ ?

#### 3.1 RHIC data

A system created at central collisions in high energy heavy-ion experiments is well described by the grand partition function  $Z(T, \mu)$  with temperature  $T$  and chemical potential  $\mu$ . Equation (2.2) means that an event with baryon multiplicity  $n$  occurs with a probability proportional to  $Z_n \xi^n$ ,

$$P_n(\xi) = Z_n \xi^n. \quad (3.1)$$

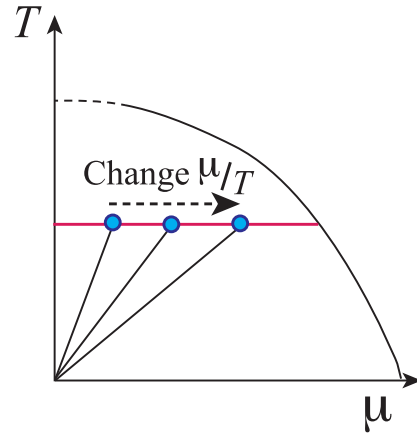


**Figure 3:** From the relation  $Z(T, \mu) = \sum_n Z_n(T) (e^{\mu/T})^n$ , we can get the information at different values of  $\mu/T$  at fixed  $T$ .

Using Eqs.(2.3) and (3.1), we can determine both  $\xi$  and  $Z_n$  from experimental data. Currently, experimental data on the net baryon multiplicity are not available, and we employ the net proton multiplicity data of Refs. [1, 2] instead. We assume that they have similar behavior. Here we use the data with the centrality 0 - 5% and analyze the multiplicities at  $\sqrt{s_{NN}} = 11.5, 19.6, 27, 39, 64.4$  and 200 GeV.

Figure2 shows the obtained  $\xi$  together with that obtained by freeze-out analysis in Ref.[4]. Note that the freeze-out temperature and chemical potential in Ref.[4] were obtained from secondary particle distributions and yields, and multiplicity was not used. Some of the obtained  $Z_n$  are shown in Fig.2.

### 3.2 Lattice QCD

#### Fugacity expansion method

Lattice QCD simulations are usually performed using the grand partition functions

$$Z(\mu, T) = \int \mathcal{D}U (\det \Delta(\mu))^{N_f} \exp(-S_G), \quad (3.2)$$

where  $\Delta$  is the matrix for Wilson fermions and  $S_G$  is the gluon action. To reduce the lattice discretization artifacts, some improvements are made to  $\Delta$  and  $S_G$  in this study.  $\Delta$  is expressed by the reduction formula developed in Ref.[7],

$$\det \Delta(\mu) = C_0 \xi^{-N_{\text{red}}/2} \prod_{n=1}^{N_{\text{red}}} (\lambda_n + \xi) = C_0 \sum_{n=0}^{N_{\text{red}}} c_n \xi^{n-N_{\text{red}}/2} = C_0 \sum_{n=-N_{\text{red}}/2}^{N_{\text{red}}/2} c_n \xi^n, \quad (3.3)$$

where  $\lambda_n$  are the eigenvalues of the reduced matrix and  $N_{\text{red}} = 4N_c N_x N_y N_z$ , with the number of colors  $N_c$  and lattice spatial size  $N_x N_y N_z$ . We substitute Eq.(3.3) into Eq.(3.2), and then the  $Z_n$  are obtained from Eq.(2.2).

#### Hasenfratz-Toussant method

Another way is the Fourier transformation of the grand partition function as a function of the imaginary chemical potential [8],

$$Z_n(T) = \int \frac{d\theta}{2\pi} e^{i\theta n} Z(\theta \equiv \frac{Im\mu}{T}, T). \quad (3.4)$$

We employ the reweighting method

$$Z_n(T) = \int \frac{d\theta}{2\pi} e^{i\theta n} \frac{\det \Delta(\theta)}{\det \Delta(\theta_0)} \det \Delta(\theta_0) \exp(-S_G). \quad (3.5)$$

In order to estimate  $\det \Delta$ , we use the hopping parameter expansion,

$$\det \Delta = \det(I - \kappa Q) = \exp \text{Tr} \log(I - \kappa Q) = \exp \text{Tr} \sum_m \frac{1}{m} \kappa^m Q^m \quad (3.6)$$

Since the chemical potential accompanies to the link variables along the temporal direction as  $e^\mu U_4(x)$  and  $e^{-\mu} U_4^\dagger(x)$ , the last term of Eq.(3.6) is recombined as  $\sum_n A_n \exp(n\mu/T)$ . Then

$$Z_n = \langle A_n \rangle. \quad (3.7)$$

Although the grand partition function  $Z(\mu, T)$  is not complex when  $\mu$  is pure imaginary, the sign problem is believed to mimic the oscillating integral of the Fourier transformation in Eq.(3.4) in the canonical approach. Indeed for large  $n$ , numerical cancellation make it hard to estimate Eq.(3.4). We circumvent this problem by the multi-precision calculation [9].

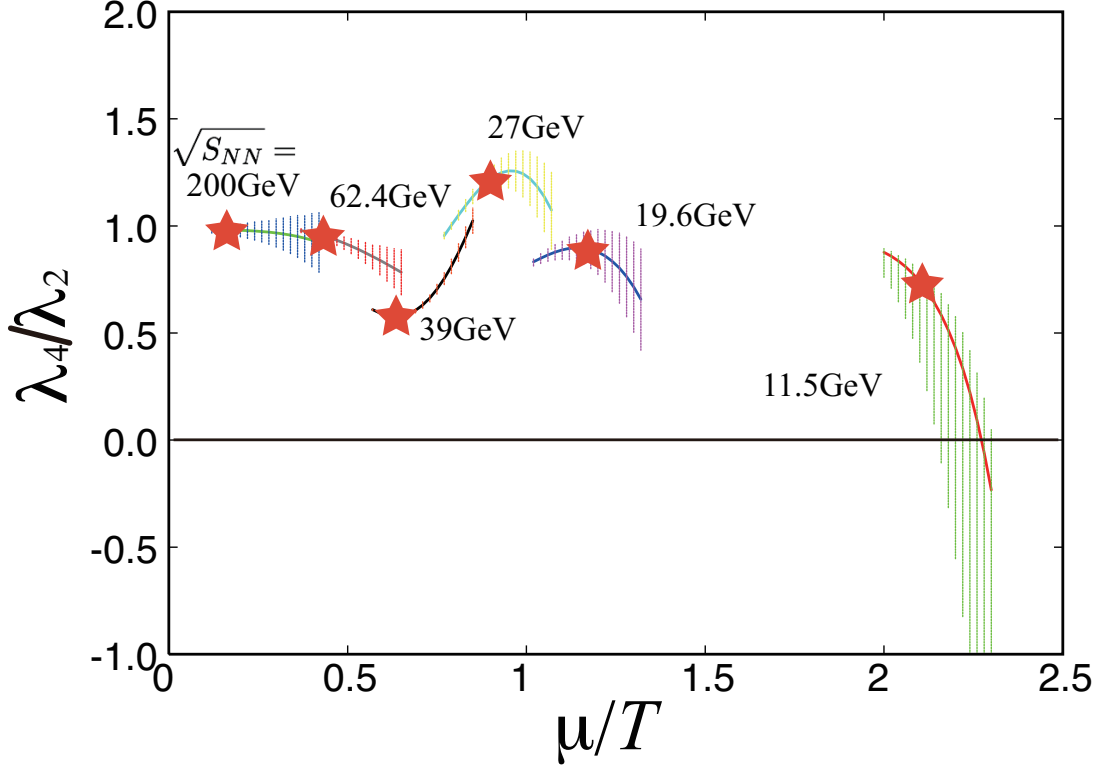


**Figure 4:**  $\lambda_4/\lambda_2$  when  $\sqrt{s_{NN}} = 11.5, 19.6, 27, 62.4$  and  $200$  GeV. The stars indicate the freeze-out points.

We compare the above two methods, and they agree very well in the regions where the hopping parameter expansion works.

## 4. Outcomes from $Z_n$

### 4.1 Moments

At first glance, the distributions of  $Z_n$  seem to be similar. However, they show very different characteristics at high and low energies. To see this feature, let us calculate the moments[10]

$$\lambda_k \equiv \left( T \frac{\partial}{\partial \mu} \right)^k \log Z. \quad (4.1)$$

for RHIC data.

In Fig.4, we show  $\lambda_4/\lambda_2$ , the so-called kurtosis. At each energy, a red star represents the point of the freeze-out, i.e., the values of  $T$  and  $\mu$  on which  $Z_n$  are estimated. We extracted the canonical partition functions  $Z_n$  in the previous section, we can predict the moments at higher  $\mu/T$ . When  $\sqrt{s_{NN}} = 19.6$  GeV,  $\lambda_4/\lambda_2$  becomes negative when  $\mu/T$  increases; this behavior may indicate a phase transition[11],[12].

## 4.2 Lee-Yang zeros

Once we obtain  $Z_n$ , Eq.(2.2) allows us to calculate  $Z(T, \xi)$ , even for complex values of the fugacity  $\xi$ . The zeros of grand canonical partition functions in the complex fugacity plane,  $Z(\alpha) = 0$ , are known as Yang-Lee zeros[13]. Their structure reflects the critical nature of the system. If the zeros form a line and cross the real  $\xi$  axis, it is the first phase transition point.

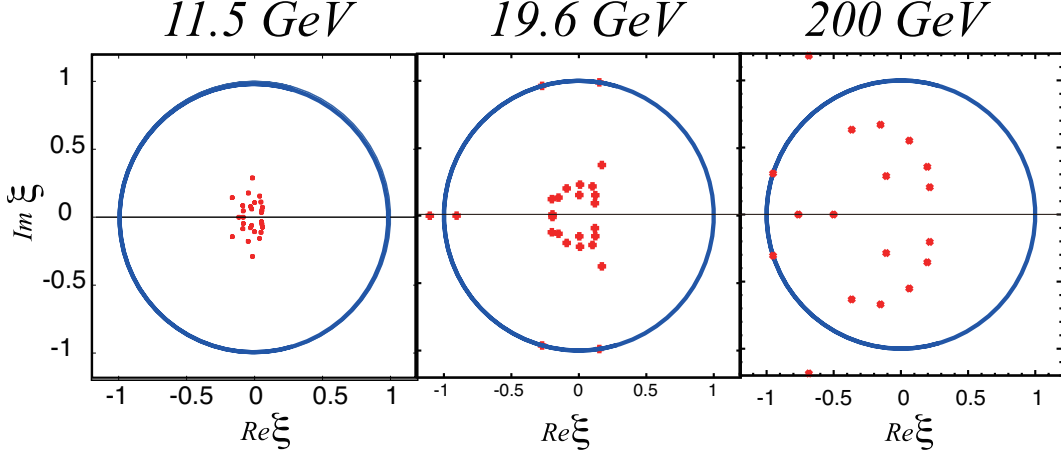


**Figure 5:** Yang-Lee zero diagram of RHIC data when  $\sqrt{s_{NN}} = 11.5, 19.6$  and  $200$  GeV.

We show Yang-Lee zero diagrams obtained from RHIC data when  $\sqrt{s_{NN}} = 11.5, 19.6$  and  $200$  GeV in Fig.5. To observe the behavior at the large-volume limit, we require higher- multiplicity data or a model that can be used to safely extrapolate the data.

In Fig.6, the Yang-Lee zero diagram calculated by lattice QCD simulation is depicted. In this diagram we see a clear signal of the Roberge-Weiss phase transition [14], which appears not only in the pure imaginary chemical potential region ( $|\xi| = 1$ ) but also spreads along the radial direction. This behavior is not seen in RHIC cases, suggesting that the RHIC data are in the confinement phase.

## 5. Concluding Remarks

In this report, we show how to construct canonical partition functions  $Z_n$  from high-energy heavy ion collision data and lattice simulation data. Using Eq.(2.2), we can predict denser regions in the QCD phase diagram. This increases the power of BES (beam energy scan) to search for QCD phase transition regions, because now an experiment at a fixed energy can prove extended regions in the QCD phase diagram.

From the relation,  $Z(\mu, T) = \sum Z_n \xi^n$  with  $\xi = e^{\mu/T}$ ,  $Z_n$  of large  $n$  regions contribute for  $\mu > T$ , i.e.,  $\xi > 1$ , although  $Z_n$  decreases rapidly. Therefore, to investigate large  $\mu$  area, we must estimate  $Z_n$  of large  $n$  very accurately.

Usually higher moments are used as an indicator of proximity to the phase transition. In the proposed method, we employ all the available  $Z_n$  to obtain information. More analyses will be required to obtain reliable error bars for calculated moments and Yang-Lee zeros.  $N_{max}$  in

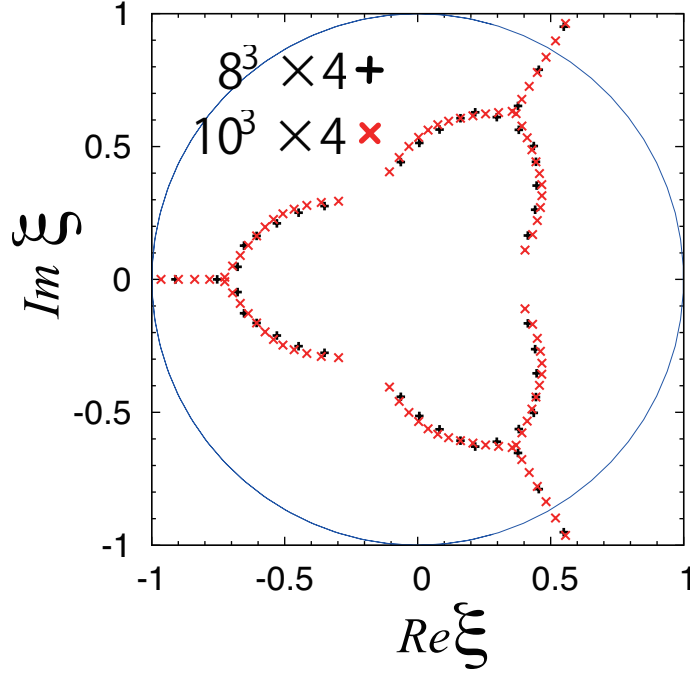


**Figure 6:** The Yang-Lee zero diagram calculated in lattice QCD simulations. Two simulations on different space sizes give consistent results, when the number densities are roughly same.

Eq.(2.2) is much smaller than the kinematically allowed values in both RHIC experimental data and the lattice QCD; in other words the contribution of higher values of  $n$  are missing. Since these contributions correspond to higher densities, our prediction of the critical chemical potential  $\mu_c$  should be considered as a lower limit.

Our data are not enough both experimental and lattice QCD cases to determine the QCD phase structure at the moment. More explicitly,  $N_{max}$  in Eq.2.2 is not large enough. We expect effective models to complement the shortage. As the first trial, let us see whether the bifurcation often seen in the lattice simulation has the physical meaning. We consider the chiral random matrix model with  $N_s$  sites given in [15],

$$Z_{\text{RM}} = \int \mathcal{D}X \exp\left(-\frac{N_s}{\sigma^2} \text{Tr}XX^\dagger\right) \det^{N_f}(D+m) \quad (5.1)$$

where  $D$  is the  $2N_s \times 2N_s$  matrix approximating the Dirac operator. It takes the form

$$D = \begin{pmatrix} 0 & iX + iC \\ iX^\dagger + iC & 0 \end{pmatrix}. \quad (5.2)$$

The matrix  $C$  includes terms to describe the effect of temperature and chemical potential. We extend the model to exhibit the appropriate periodicity. We set  $N_s = 60$ . In this case  $N_{max} = N_s = 60$ . In Fig.7, the Lee-Yang zeros for  $N_{max} = 60, 58$  and  $56$  cases are shown. No bifurcation appears at  $N_{max} = 60$ , i.e., in the exact case, while it appears when we truncate  $Z_n$  for  $N \geq N_{max}$ . Although the “volume”  $N_s$  is finite and therefore the model does not have Lee-Yang zero on the real axis, this

suggests that the bifurcation seen in the lattice simulations at large (real) chemical potential regions is due to the truncation effect.

We believe now that the canonical approach is very useful and promising both for experimental and lattice QCD researches at finite density. One difficulty is its application at low temperature where  $\mu/T$  is very small, and consequently we need to calculate  $Z_n$  very precisely until very large  $n$ . Below the transition temperature,  $Z_n$  is more difficult than above the transition temperature. In the hopping parameter method, it is understandable because  $A_n$  in Eq.(3.7) is a kind of extended Polyakov loop, which is small under the phase transition temperature.

This difficulty under the transition temperature occurs also in the fugacity expansion method. The reason is unclear.

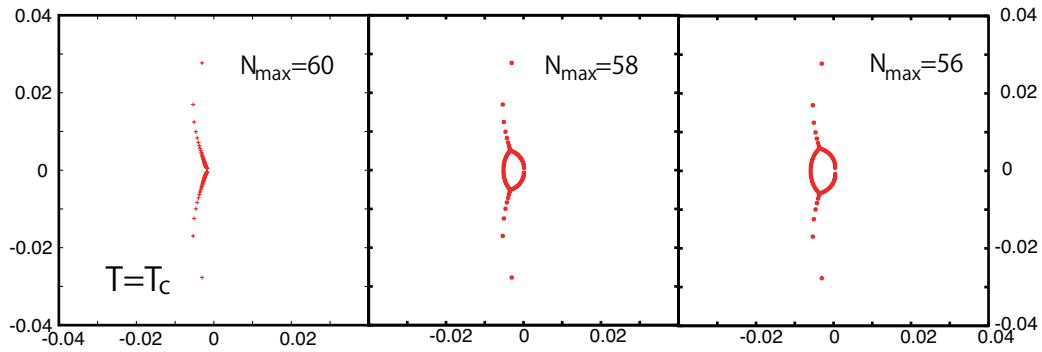


**Figure 7:** Effects of truncation of  $Z_n$ .

## References

- [1] M.M. Aggarwal et al., Phys. Rev. Lett. **105** (2010) 022302.
- [2] X. Luo, Quark Matter 2012 Nucl. Phys. A 904-905, (2013) 911c.
- [3] K. Fukushima and T. Hatsuda, Rept. Prog. Phys. 74:014001, 2011.
- [4] J.Cleymans et al., Phys. Rev. C73, (2006) 034905.
- [5] Ph. de Forcrand PoS (LAT2009)010, 2009.
- [6] P. Braun-Munzinger, K. Redlich and J. Stachel, Quark Gluon Plasma 3, 491, Eds. R. Hwa and X.N. Wang, World Scientific, Singapore, 2004.
- [7] K. Nagata and A. Nakamura, Phys. Rev. D82 (2010) 094027.
- [8] A. Hasenfratz, D. Toussaint, Nucl. Phys. B371, 539 (1992).
- [9] D. M. Smith, <http://myweb.lmu.edu/dmsmith/FMLIB.html>
- [10] K. Redlich, Central Eur. J. Phys. 10 (2012) 1254.
- [11] K.Morita et al., Eur.Phys.J. C74 (2014) 2706.
- [12] B. Friman et al., Euro. Phys. J C(2011) 71: 1694.
- [13] C. N. Yang and T. D. Lee, Phys. Rev. **87**, 404 (1952), T. D. Lee and C. N. Yang, Phys. Rev. **87** (1952) 410.

- [14] A. Roberge and N. Weiss, Nucl. Phys. B275(1986) 734.
- [15] M. A. Halasz, A. D. Jackson, R. E. Shrock, M. A. Stephanov, and J. J. M. Verbaarschot, Phys. Rev. D 58, 096007 (1998).